

# Polarized photons in radiative muon capture

Shung-ichi Ando<sup>a†</sup>, Harold W. Fearing<sup>b‡</sup>, and Dong-Pil Min<sup>c§</sup>

<sup>a</sup> *Department of Physics and Astronomy, University of South Carolina, Columbia, SC 29208, USA*

<sup>b</sup> *TRIUMF, 4004 Wesbrook Mall, Vancouver, British Columbia, Canada V6T 2A3*

<sup>c</sup> *School of Physics and Center for Theoretical Physics, Seoul National University, Seoul 151-742, Korea*

(April 24, 2001)

We discuss the measurement of polarized photons arising from radiative muon capture. The spectrum of left circularly polarized photons or equivalently the circular polarization of the photons emitted in radiative muon capture on hydrogen is quite sensitive to the strength of the induced pseudoscalar coupling constant  $g_P$ . A measurement of either of these quantities, although very difficult, might be sufficient to resolve the present puzzle resulting from the disagreement between the theoretical prediction for  $g_P$  and the results of a recent experiment. This sensitivity results from the absence of left-handed radiation from the muon line and from the fact that the leading parts of the radiation from the hadronic lines, as determined from the chiral power counting rules of heavy-baryon chiral perturbation theory, all contain pion poles.

PACS numbers: 23.40.-s, 12.39.Fe, 24.70.+s

## I. INTRODUCTION

The first measurement of radiative muon capture (RMC) on hydrogen,

$$\mu^- + p \rightarrow \nu_\mu + n + \gamma, \quad (1)$$

has been reported by a TRIUMF group [1], and the value of the induced pseudoscalar constant  $g_P$  was deduced to be about 1.5 times larger than that predicted by the partially conserved axial current (PCAC) or that obtained from one-loop order heavy-baryon chiral perturbation theory (HBChPT) calculations [2,3]. In Ref. [4] the photon spectrum from RMC on a proton was obtained within the context of HBChPT up to next-to-next-to leading order (NNLO), i.e., to one loop order. The results simply confirm a next-to-leading order (NLO) HBChPT calculation [5] and the earlier theoretical predictions [6–10] based on a phenomenological tree-level Feynman graph approach. Furthermore, the results of Ref. [4] indicated that the chiral series converges rapidly, and thus suggest that the discrepancy between experiment and theory observed for RMC on a proton cannot be explained by higher order corrections within HBChPT. Since then, many analyses have been reported, incorporating a variety of new elements and suggestions, but all have essentially confirmed earlier results and concluded that the existing discrepancy is still unexplained [11–15].<sup>1</sup>

As it appears that a NNLO calculation which includes all diagrams through one-loop order converges sufficiently, the only possibilities for significant improvement would seem to come from effects outside the context of HBChPT, or perhaps from terms originating in the Wess-Zumino Lagrangian. These Wess-Zumino terms turn out to be negligible however, as shown in Ref. [11]. Furthermore, all possible expressions in the amplitude which can be composed of the characteristic operators involved in the reaction, namely the polarization vectors of the photon and the lepton current, the three-momenta of the outgoing photon and of the exchanged weak vector boson, and the spin operator of the

---

<sup>†</sup>E-mail address : [sando@nuc003.psc.sc.edu](mailto:sando@nuc003.psc.sc.edu)

<sup>‡</sup>E-mail address : [fearing@triumf.ca](mailto:fearing@triumf.ca)

<sup>§</sup>E-mail address : [dpmi@snu.ac.kr](mailto:dpmi@snu.ac.kr)

<sup>1</sup>A sea-gull term was introduced in the RMC amplitude in Ref. [16], which could reproduce the experimental data. However, it was shown [17] that this term was not gauge invariant and in addition that it was already present, together with the additional pieces needed for gauge invariance, in the HBChPT approach of Ref. [4] and in the standard Feynman graph method of e.g. Ref. [7].

nucleon, emerge already in the one-loop order. Therefore, higher order contributions in the HBChPT perturbation series will give corrections only to the coefficients of these operator expressions and should be small, in view of the rapid convergence of the chiral series in this reaction. This led us to the conclusion that something other than the ingredients of the hadronic vertices may in fact be the source of the problem. For example, there may be difficulties in our understanding of the atomic and molecular states of the muonic atom in hydrogen. In particular the dependence of the photon spectrum on the initial muonic atom states is non-negligible, so that it is important to try to find a quantity which is less sensitive to the atomic and molecular states but, at the same time, is sensitive to the pseudoscalar constant.

Quite recently, some alternative scenarios for possible resolution of the “ $g_P$  puzzle” have been suggested by two groups. In Ref. [18], the photon spectrum corresponding to the experiment of Ref. [1] was fitted by adjusting a parameter  $\xi$ , with  $(1 - \xi)$  giving the fraction of spin 3/2 ortho  $p$ - $\mu$ - $p$  molecular state in liquid hydrogen. A value  $\xi = 0.8 \sim 0.9$  was obtained, which is smaller than the theoretical prediction  $\xi = 1$  [19,20] and would correspond to a 10 to 20 % component of the spin 3/2 state <sup>2</sup>. In Ref. [14], on the other hand, the authors speculate that the “ $g_P$  puzzle” can be explained by accumulation of small effects and variations of parameters, or perhaps by an isospin breaking effect.

As we have observed, the present situation viewed from the context of HBChPT can be summarized as follows. All symmetries of QCD are respected order by order in this theory and the chiral expansion is rapidly converging. The rapid convergence is fortunate, since to improve the theory by calculating higher orders would require including all of the many possible diagrams of the chiral order under consideration and would normally introduce a large number of new low energy constants which would have to be constrained by experiments. Furthermore, the HBChPT results agree fairly well with those obtained from the standard diagram approach, so that all theoretical approaches are reasonably consistent, and unable to explain the RMC data with the predicted value of  $g_P$ .

It is probably important to remeasure the photon spectrum in RMC, or to measure more precisely the rate for ordinary muon capture (OMC),  $\mu + p \rightarrow \nu + n$ , as has been proposed [24]. Alternatively, one could consider performing a rather more sophisticated experiment which would be sensitive to some different combination of the ingredients of the problem. In that vein, we want to propose here to measure the polarization of the outgoing photon.

Measuring the photon polarization enables us to choose the most important graphs which involve pion poles and therefore to enhance the dependence of the result on the pseudoscalar coupling constant  $g_P$ . In the usual transverse gauge<sup>3</sup> by far the most important diagram for RMC is the one where the photon is emitted from the leptonic current. The pseudoscalar coupling constant is an important contributor to this diagram, since  $g_P$  is so much larger than  $g_V$  or  $g_A$ , but its importance is not enhanced by the pion pole because the momentum transfer in this diagram is always spacelike. Therefore, to concentrate on the pseudoscalar constant, we would like to find the channel where this diagram is blocked. The polarization experiment blocks this channel.

The rationale is simple and transparent. Since the neutrino is left-handed, the photon emitted from the leptonic current is right-handed. This was shown for V and A couplings in Ref. [25] and generalized to include the induced couplings as well in Ref. [26]. A measurement of a left-handed photon filters out the photon from the leptonic current, and is thus sensitive to radiation from the hadronic current. The sensitivity to  $g_P$  comes from the fact that some parts of the hadronic current, and in particular some parts containing pion poles, are of leading order by the power counting rules of HBChPT.

The photon circular polarization in RMC (to be defined explicitly below) has been considered before in the context of a phenomenological treatment of the weak nucleon current parameterized by form factors [26]. There it was shown that the circular polarization (and also the photon asymmetry relative to the muon spin) could be written as  $1 + \mathcal{O}(1/m_N^2)$  where  $m_N$  is the nucleon mass and where the coefficient of the  $\mathcal{O}(1/m_N^2)$  term involves the various coupling constants. We will discuss below the expansion scheme in powers of  $1/m_N^2$  corresponding to this theorem and its connection to the power counting scheme of HBChPT.

---

<sup>2</sup>The authors of Ref. [18] also considered ordinary, non radiative muon capture (OMC) and originally found there the same value of  $\xi$  found for RMC. That result was obtained however using a formula relating the liquid hydrogen and ortho molecular rates which did not correspond to the experimental conditions of the OMC experiment [21]. Using an appropriate formula [22,23] one finds that  $\xi = 1$  results in a value which is in good agreement with the OMC data. However if one considers the uncertainties in the data and in some of the parameters one finds that values of  $\xi$  as small as  $\xi \sim 0.9$  are possible, which is consistent, but only marginally so, with the result found for RMC.

<sup>3</sup>Note that individual diagrams are not gauge invariant by themselves, so any comments about relative sizes are gauge dependent. We will always assume the transverse gauge for any such comparisons.

The Feynman graphs contributing to RMC on a proton can be classified into the two classes shown in Fig. 1: (a) the first corresponds to those graphs where the muon radiates, and (b) the second to the graphs where the hadron radiates. The amplitude of the process can then be written as the sum of two diagrams,

$$M_{fi} = \frac{eG_F V_{ud}}{\sqrt{2}} \epsilon_\alpha^* [\mathcal{M}^{\alpha\beta} J_\beta + \mathcal{J}_\beta M^{\alpha\beta}], \quad (2)$$

where  $e$  is the electric charge,  $G_F$  is the Fermi constant,  $V_{ud}$  is a Kobayashi-Maskawa matrix element, and  $\epsilon_\alpha^*$  is the polarization vector of photon. The hadron matrix elements with three and four legs are denoted by  $J_\beta$  and  $M_{\alpha\beta}$ . Their properties have been studied in Ref. [4], and are briefly discussed in the next section.

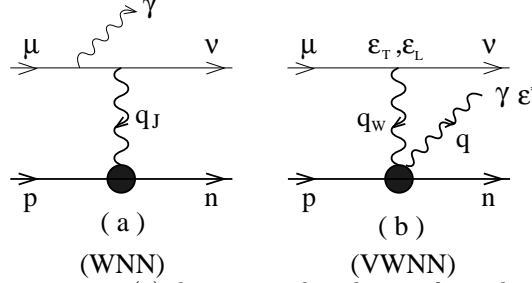


FIG. 1. Diagrams for radiative muon capture; (a) diagram with radiation from the muon line. The matrix element of the weak nucleon current  $J_\beta$  is matched with the lepton matrix element  $\mathcal{M}^{\alpha\beta}$ . (b) diagram with radiation from the hadronic current whose matrix element  $M_{\alpha\beta}$  is matched with the lepton matrix element  $\mathcal{J}_\beta$ .

The lepton matrix elements with three and four legs,  $\mathcal{J}_\beta$  and  $\mathcal{M}_{\alpha\beta}$  are given by

$$\mathcal{J}_\beta = \bar{u}_\nu \gamma_\beta (1 - \gamma_5) u_\mu, \quad (3)$$

$$\mathcal{M}_{\alpha\beta} = \bar{u}_\nu \gamma_\beta (1 - \gamma_5) \frac{\gamma \cdot (\mu - q) + m_\mu}{2\mu \cdot q} \gamma_\alpha u_\mu, \quad (4)$$

where  $\mu$  ( $q$ ) is four momentum of muon (photon),  $m_\mu$  is the muon mass, and  $u_\mu$  ( $u_\nu$ ) is the Dirac spinor for the muon (neutrino).

First, we study the lepton matrix elements involving a polarized photon. In the laboratory frame we assume that the  $z$ -axis of our coordinate system coincides with the neutrino direction and the  $x$ - $z$  plane includes the photon trajectory. Thus we have

$$\hat{\nu} = (0, 0, 1), \quad \hat{q} = (\sin \theta, 0, \cos \theta), \quad (5)$$

where  $\hat{\nu}$  ( $\hat{q}$ ) is the unit vector of the neutrino (photon) momentum and  $\theta$  is the angle between neutrino and photon,  $\hat{\nu} \cdot \hat{q} = \cos \theta$ . In the transverse (Coulomb) gauge the polarization vectors of the photon are given by

$$\vec{\epsilon}_L^* = \frac{1}{\sqrt{2}}(-\cos \theta, -i, \sin \theta), \quad \vec{\epsilon}_R^* = \frac{1}{\sqrt{2}}(\cos \theta, -i, -\sin \theta), \quad (6)$$

where subscripts  $L$  and  $R$  stand for the left- and right-handed polarization state, respectively. In this frame we can rewrite Eqs. (3) and (4) in terms of components of four vectors for each spin state,

$$\mathcal{J}^\beta(+) \equiv \epsilon_T^\beta = 2\sqrt{2m_\mu E_\nu}(0, -1, -i, 0), \quad (7)$$

$$\mathcal{J}^\beta(-) \equiv \epsilon_L^\beta = 2\sqrt{2m_\mu E_\nu}(1, 0, 0, 1), \quad (8)$$

$$\mathcal{M}^\beta(+, R) = 2\sqrt{\frac{E_\nu}{m_\mu}}(1 + \cos \theta, \sin \theta, i \sin \theta, 1 + \cos \theta), \quad (9)$$

$$\mathcal{M}^\beta(-, R) = 2\sqrt{\frac{E_\nu}{m_\mu}}(\sin \theta, 1 - \cos \theta, i(1 - \cos \theta), \sin \theta), \quad (10)$$

$$\mathcal{M}^\beta(\pm, L) = 0, \quad (11)$$

where  $\mathcal{M}^\beta(\pm, h) \equiv \epsilon_{h,\alpha}^* \mathcal{M}^{\alpha\beta}(\pm, h)$ . Signs  $(\pm)$  and  $h=(R, L)$  in the parenthesis of l.h.s. of the equations denote, respectively, up and down muon spin state along the  $z$ -axis, and right- and left-handed photon polarization state<sup>4</sup>. Eqs. (9), (10), and (11) show that the photons radiated from the muon line are totally right-handed polarized [25,26].

If one measures the left-handed photons, the amplitude of Eq. (2) is reduced to

$$M_{fi}^{(L)} = \frac{e G_F V_{ud}}{\sqrt{2}} \mathcal{J}_\beta M^\beta(L), \quad (12)$$

where  $M^\beta(L) \equiv \epsilon_{L,\alpha}^* M^{\alpha\beta}$  is the part of  $M^{\alpha\beta}$  producing only left-handed photons, where the spin indices of proton and neutron are suppressed.

Therefore we can investigate the part of the hadron four-point matrix element  $M^\beta(L)$  which produces left-handed photons, without the interference of the lepton radiating diagram containing the weak nucleon current  $J_\beta$ , by measuring the left circularly polarized photons. The circular polarization  $\beta$ , which is defined by

$$\beta \equiv \frac{N^R - N^L}{N^R + N^L} \quad (13)$$

where  $N^R$  ( $N^L$ ) is the spectrum of right-handed (left-handed) photons<sup>5</sup>, has the property that  $\beta = 1$  for the muon radiating diagram of Fig. 1 (a) [25,26]. Therefore, for  $\beta = 1 + \Delta\beta$ , the deviation from one,  $\Delta\beta = -2N^L/(N^L + N^R)$ , should come entirely from the contribution of  $M^\beta(L)$ .

### III. CHIRAL COUNTING RULE AND HADRON MATRIX ELEMENTS OF RMC

HBChPT [28] is a low energy effective field theory of QCD, which has a systematic expansion scheme in terms of  $Q/\Lambda_\chi$ , where  $Q$  is a typical four-momentum scale characterizing the process in question,  $\Lambda_\chi$  is the chiral scale with  $\Lambda_\chi \simeq 4\pi f_\pi \sim m_N \simeq 1$  GeV, and where  $f_\pi$  is the pion decay constant.  $Q$  must be small, typically of the order of the pion mass  $m_\pi$ . A typical scale  $Q$  in muon capture (both OMC and RMC) is the muon mass  $m_\mu = 105.7$  MeV, and hence  $Q/\Lambda_\chi \simeq 0.1$ . One therefore expects a rapid convergence of relevant chiral perturbation series for muon capture and the explicit HBChPT calculations are consistent with this expectation [2–5,14,18].

The effective Lagrangian is expanded as

$$\mathcal{L} = \sum \mathcal{L}_{\bar{\nu}} = \mathcal{L}_0 + \mathcal{L}_1 + \mathcal{L}_2 + \cdots, \quad (14)$$

where the subscript  $\bar{\nu}$  denotes the order of terms,  $\bar{\nu} = d + n/2 - 2$ , with  $n$  the number of nucleon lines and  $d$  the number of derivatives or powers of  $m_\pi$  involved in a vertex.  $\mathcal{L}_0$ ,  $\mathcal{L}_1$ , and  $\mathcal{L}_2$  are the leading order (LO), next-to leading order (NLO), and next-to-next-to leading order (NNLO) parts of the Lagrangian, respectively, and their explicit form has been given in Ref. [4]. In passing, we should note that the  $\mathcal{L}_1$  includes the terms of  $\mathcal{O}(1/m_N)$  which are corrections to the leading order Lagrangian. In the NNLO Lagrangian we have seven unknown constants, the so-called *low energy constants* (LEC's), which are not determined by symmetry but must be fixed by experiments. Three of the seven LEC's appear in the three point vertex functions of  $J_\beta$ , and they are fixed by the vector and axial vector radius and the Goldberger-Treiman discrepancy [3,4,14,18]. One of the remaining four constants is fixed via a rare pion decay [29], and the remaining three constants are estimated using the  $\Delta(1232)$  and  $\rho$  saturation method [30].<sup>6</sup> Therefore there are no undetermined parameters in the calculation.

---

<sup>4</sup>We define the polarization vectors for the lepton current,  $\varepsilon_T^\beta$  and  $\varepsilon_L^\beta$ , as depicted in Fig. 1, via Eqs. (7) and (8).

<sup>5</sup>The unpolarized spectrum  $d\Gamma/dE_\gamma$  is obtained by  $d\Gamma/dE_\gamma = N^R + N^L$ .

<sup>6</sup>Recently, these LEC's have been determined using data for radiative pion capture [31] and employing the Lagrangian of Ecker and Mojžiš [32].

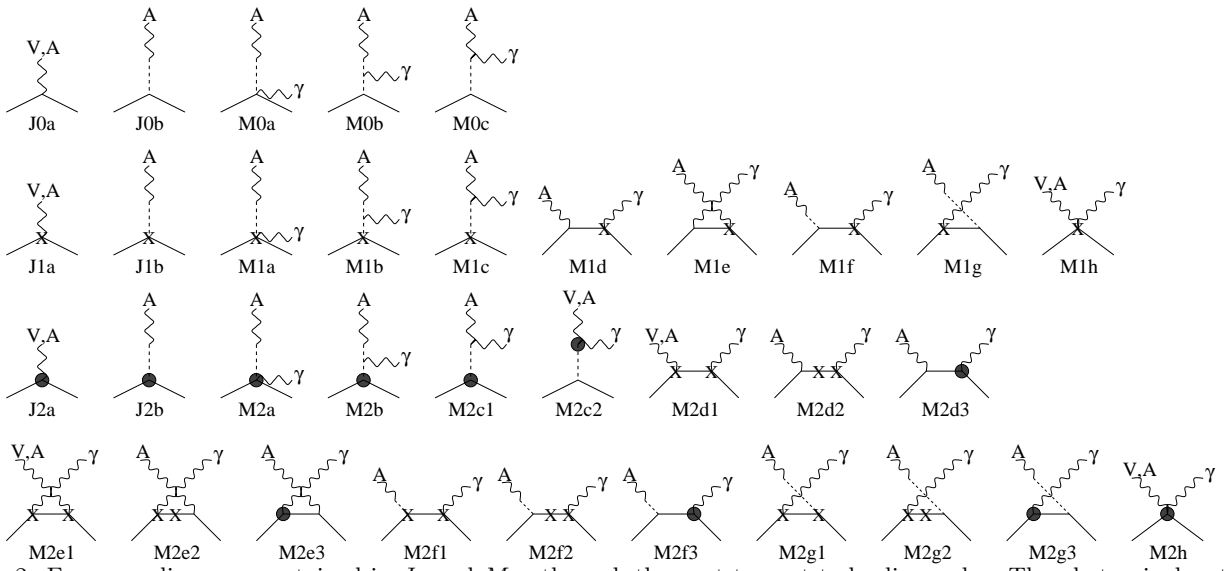


FIG. 2. Feynman diagrams contained in  $J_\beta$  and  $M_{\alpha\beta}$  through the next-to-next-to leading order. The photon is denoted by  $\gamma$ , the weak current is decomposed into  $V, A$  parts, and a dashed line denotes an exchanged pion. Vertices without blobs are from  $\mathcal{L}_0$ , those with “X” are from  $\mathcal{L}_1$  and those with “•” are from  $\mathcal{L}_2$  or the one-loop corrections. The five diagrams in the first line are diagrams of LO, which originate from  $\mathcal{L}_0$ . The next ten diagrams in the second line are those of NLO, which contain one “X” of  $\mathcal{L}_1$ . The following 19 diagrams in the third and forth lines are those of NNLO, which contain two “X”s of  $\mathcal{L}_1$  or one “•” of  $\mathcal{L}_2$  or a one-loop correction.

Let us look at the diagrams involving the hadron matrix elements  $J_\beta$  and  $M_{\alpha\beta}$  in Fig. 2. (See the caption of the figure for more details.) The LO, NLO, and NNLO diagrams are drawn in the first line, the second line, and the third and fourth lines in Fig. 2, respectively. Since, as noted earlier [4], the series converges well, we expect those diagrams in the first line to be the most important. Both left- and right-handed photons are emitted from the hadron matrix element  $M_{\alpha\beta}$ , and all the leading order diagrams of  $M_{\alpha\beta}$  (M0a, M0b, M0c) contain a pion pole.

Observe that two different momentum transfers appear in the pion poles in the M0 diagrams. For M0c and the lower pole of M0b, the momentum transfer  $q_J = \mu - \nu - q$  is relevant.  $q_J^2$  is always spacelike, has no significant  $E_\gamma$  dependence, and is generally  $\sim -m_\mu^2$ . On the other hand for the M0a diagram and the upper pole of M0b the relevant momentum transfer is  $q_W = \mu - \nu$ . This depends on  $E_\gamma$  via  $q_W^2 \simeq 2m_\mu E_\gamma - m_\mu^2$  and becomes  $\sim +m_\mu^2$  near the upper end of the photon spectrum. Thus one is much closer to the pion pole for these diagrams. This means that, other factors being equal, these diagrams will be enhanced relative to those involving  $q_J$ .

Now let us discuss the theorem of Ref. [26] and the connection between the standard Feynman diagram approach to RMC and the HBChPT approach described here. In HBChPT the most important diagram contributing to the hadronic pieces of Fig. 2 is the seagull diagram, M0a. This is just the standard Kroll-Ruderman term, which however is not explicitly seen in the diagrams of the relativistic phenomenological model (Fig. 1 of Ref. [7]), since that model used a pseudoscalar pion-nucleon coupling. Had pseudovector coupling been used it would have appeared explicitly. It can however be directly identified as part of the diagram  $M_b$  in Fig. 1 (b) of Ref. [7] where the photon radiates from proton, the proton propagates, and interacts with the lepton current, where the vertex of the weak nucleon current is described by the weak form factors. The M0a diagram is included in the contribution from the negative energy propagation of the proton in the  $M_b$  diagram. (M0b and M0c can be also identified as parts of (d) and (e) in Fig. 1 of Ref. [7], respectively.)

In the phenomenological model the amplitude  $M_b$  can be expanded in terms of  $1/m_N$  as

$$\begin{aligned}
M_b = \frac{1}{2m_N} \chi_n^\dagger \Big\{ & g_V \left[ \vec{\epsilon}^* \cdot \vec{\mathcal{J}} + (1 + \kappa_p) \mathcal{J}^0 i \vec{\sigma} \cdot \vec{\epsilon}^* \times \hat{q} - i \vec{\sigma} \cdot \vec{\epsilon}^* \times \vec{\mathcal{J}} \right] \\
& + g_A \left[ \mathcal{J}^0 \vec{\sigma} \cdot \vec{\epsilon}^* - (1 + \kappa_p) (i \hat{q} \cdot \vec{\epsilon}^* \times \vec{\mathcal{J}} + \vec{\sigma} \cdot \vec{\epsilon}^* \hat{q} \cdot \vec{\mathcal{J}} - \vec{\sigma} \cdot \hat{q} \vec{\epsilon}^* \cdot \vec{\mathcal{J}}) \right] \\
& + g_P(q_W) \frac{q_W \cdot \vec{\mathcal{J}}}{m_\mu} \vec{\sigma} \cdot \vec{\epsilon}^* \Big\} \chi_p + \mathcal{O}(1/m_N^2),
\end{aligned} \tag{15}$$

where the nucleon weak form factors are denoted by  $g_V$  for vector,  $g_A$  for axial vector, and  $g_P(q_W)$  for pseudoscalar form factors.  $\kappa_p$  is the proton anomalous moment. We confirm the result of the theorem [26] that all the terms in Eq.

(15) are  $1/m_N$  corrections. In this approach the form factors are phenomenological parameters. The  $g_P$  dependent term is formally of order  $1/m_N$ , but the form factor  $g_P$  happens to be numerically large.

The connection to the HBChPT approach can be made via the Goldberger-Treiman relation which tells us that the pseudoscalar form factor has the structure due to pion propagation, i.e. a pion pole, and is given explicitly by  $g_P(q^2) = 2m_\mu m_N g_A / (m_\pi^2 - q^2)$ . In HBChPT this expression, rather than  $g_P$ , will appear in all the pion pole terms and the  $m_N$  in the numerator will cancel the  $m_N$  appearing in the denominator, thus pushing this term to one lower order in the expansion than it is in the expansion of the phenomenological relativistic model [26].

We are now in a position to discuss what is known regarding the polarization observables of the muon capture. As mentioned before, a general theorem tells us that  $\Delta\beta$  is formally  $\mathcal{O}(1/m_N^2)$  [26]. Using a phenomenological treatment of the weak nucleon current parameterized by the form factors one can show that hadron matrix elements are of order  $J_\beta = \mathcal{O}(1)$  and  $M_{\alpha\beta} = \mathcal{O}(1/m_N)$  in the  $1/m_N$  expansion [26,27]. Hence,  $N^L \sim |M^\beta(L)|^2 = \mathcal{O}(1/m_N^2)$  and the leading part of  $N^R \sim |J_\beta|^2 = \mathcal{O}(1)$  and thus  $\Delta\beta = \mathcal{O}(1/m_N^2)$  in this model. However,  $\Delta\beta$  is not particularly small, as also noted in [26], because it contains a term proportional to  $g_P^2$ , and  $g_P$  is large, as is explained in the previous paragraph.

So to summarize, one can understand the connection between the theorem derived by expansion of the relativistic phenomenological model in Ref. [26] and the corresponding HBChPT expansion by noting that there is a one to one correspondence between the  $1$ ,  $1/m_N$ , and  $1/m_N^2$  terms in the expansion of the model and the LO, NLO, and NNLO terms of HBChPT, except for the pion pole terms which appear at one lower order in HBChPT because the  $m_N$  in the numerator of  $g_P$  has been explicitly extracted.

#### IV. NUMERICAL RESULTS

In Figs. 3, 4, 5 and 6 we plot various of our results for the spectrum and circular polarization of photons, all calculated in HBChPT up to NNLO. There are two major issues to discuss. First, what is the sensitivity to  $g_P$  of the spectrum of left-handed photons and the circular polarization and, second, how sensitive are these results to uncertainties in our knowledge of the muon atomic states.

Let us first study the sensitivity of the polarization observables to the value of  $g_P$ . In Figs 3 and 4 we plot the spectrum of left-handed photons and the photon circular polarization, respectively, in the “experimental state” (6.1 % atomic hyperfine singlet state, 85.4 % ortho  $p\text{-}\mu\text{-}p$  state, and 8.5 % para  $p\text{-}\mu\text{-}p$  state) reported in Ref. [1] for the photon energy  $E_\gamma = 60$  MeV to 100 MeV. We plot three lines which are obtained by using the HBChPT up to NNLO and the relativistic phenomenological model [7] with two  $g_P$  values,  $g_P/g_P^{PCAC} = 1$  and 1.5, where  $g_P^{PCAC} \equiv g_P(-0.88m_\mu^2)$  is the Goldberger-Treiman prediction for  $g_P$  at the momentum transfer corresponding to OMC in hydrogen.

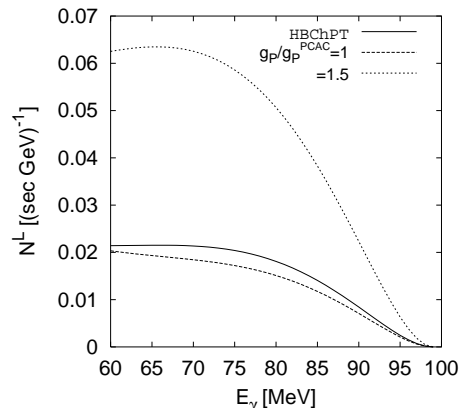


FIG. 3. The spectrum of left-handed photons in the “experimental state” is plotted for the photon energy  $E_\gamma = 60$  to 99 MeV. The solid line is the result of HBChPT up to the NNLO, and the dashed and dotted lines are results for the relativistic model [7] with two  $g_P$  values,  $g_P/g_P^{PCAC} = 1$  and 1.5, respectively.

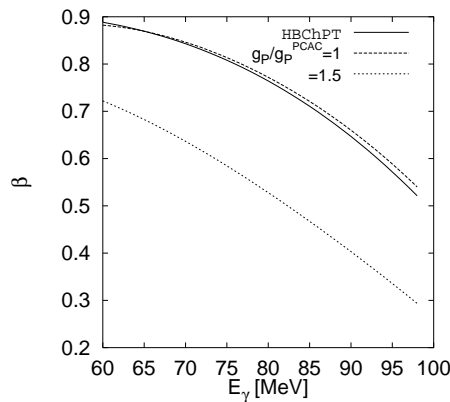


FIG. 4. Circular polarization in the “experimental state”. See the caption of Fig. 3.

One finds that the results are quite sensitive to the value of  $g_P$  as expected. The results of HBChPT and the model with  $g_P = g_P^{PCAC}$  are in good agreement in the both figures which confirms that the same basic ingredients are in both models and that the other higher order corrections in HBChPT and terms not included in the relativistic model are in fact small. The case of  $g_P/g_P^{PCAC} = 1.5$  gives a photon spectrum larger by about a factor of three than the case of  $g_P/g_P^{PCAC} = 1$ . Therefore our result shows the strong sensitivity of the polarized photon spectrum to the different values of the pseudoscalar coupling over the experimentally accessible photon energy region. This is in contrast to the unpolarized photon spectrum where the difference of photon spectra with the two different values of  $g_P$  is only of the order of 30-40% in the measurable region. The circular polarization is also sensitive and differs for the two values of  $g_P$  by a more or less constant amount 0.2 over the whole relevant region of photon energy.

Consider now the question of the sensitivity of the results to aspects of the muon’s atomic or molecular state. The photon spectrum can always be represented by a linear combination of the spectrum of singlet and that of triplet state capture. The coefficient of each state is determined by the particular target, liquid or gas, by the amount of delay between the muon stop and the beginning of counting, and by the formulas incorporating the various atomic and molecular transition rates which describe the transitions from capture, through singlet, ortho  $p\text{-}\mu\text{-}p$  and para  $p\text{-}\mu\text{-}p$  molecular states. It is known that there are some ambiguities in the parameters of these formulas, particularly with regard to the ortho-para transition rate [1] and to the possible inclusion of a spin 3/2 component in the ortho molecule [18].

In Figs. 5 and 6 we plot our results for the spectra of left- and right-handed photons, respectively, for each spin state. The solid, long-dashed, short-dashed, and dotted lines correspond to singlet, triplet, statistical, and ortho states, respectively.

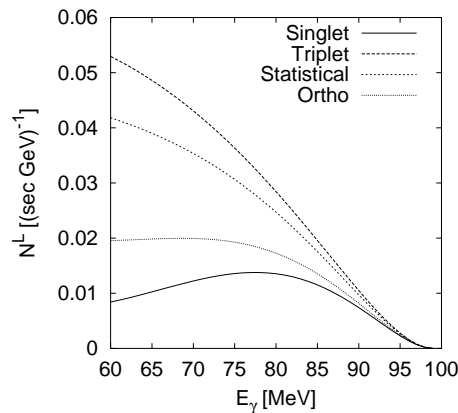


FIG. 5. The spectrum of left-handed photons is plotted for the photon energy  $E_\gamma = 60$  to 99 MeV for each spin state. The lines are the results of HBChPT up to NNLO. The solid, long-dashed, short-dashed, and dotted lines correspond to singlet, triplet, statistical, and ortho states, respectively.

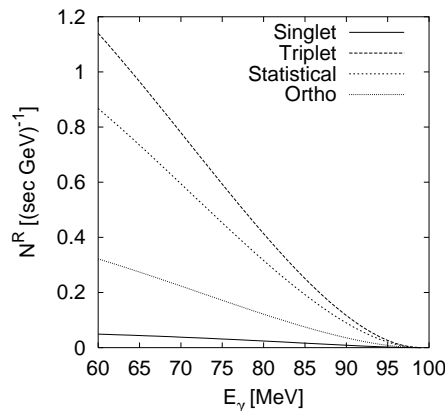


FIG. 6. The spectrum of right-handed photons for each spin state. See the caption of Fig. 5.

From these figures one can see immediately some general features. The spectrum of right-handed photons, which is also essentially the spectrum of unpolarized photons, is much larger than that for left-handed photons. Specifically by comparing the two figures we find that the rate for right-handed photons is about 2.5 times larger than that for left-handed photons for the singlet state and 17.3 times larger for the triplet state, when the spectra are integrated over the photon energy  $E_\gamma = 60$  to  $99$  MeV. Under the experimental conditions of the TRIUMF experiment [1], the ortho molecular state is dominant, so that in these conditions one would have about one-tenth as many left-handed photons as right-handed ones. Presumably this enhancement of right-handed photons is due to the strong enhancement of the triplet state and to the fact that the muon radiating diagram dominates, and, as was noted above produces purely right-handed photons.

More specifically, with regard to the question of sensitivity to the atomic and molecular states, we note that if the spectra of singlet and triplet states were the same, the relative amounts would not matter and there would be no sensitivity. From the figures we see that, while this is not the case, the singlet is in fact much more important, and closer to the triplet, for the left-handed photon case than for the right-handed one. Numerically the ratio of the singlet to triplet state spectra, when integrated over the photon energy, is 0.34 for left-handed photons and 0.05 for right-handed photons. This means that the left-handed photon case will depend less strongly on the relative amounts of singlet and triplet than the right-handed case. But one should also take into account the result above that the left-handed spectrum is much more sensitive to  $g_P$  than the right-handed (or unpolarized) spectrum. Thus one concludes that a measurement of the spectrum of left-handed photons, or equivalently the circular polarization of the photons, as we propose here, should be significantly less sensitive to the atomic and molecular ambiguities per unit of sensitivity to  $g_P$  than is the right-handed or unpolarized spectrum.

## V. SUMMARY AND DISCUSSION

We have discussed RMC on the proton in the case when the measured photon is polarized and have shown that the spectrum involving left-handed photons and the photon circular polarization are quite sensitive to the pseudoscalar coupling constant  $g_P$ . They are somewhat less sensitive than the unpolarized case to the atomic and molecular spin state as well. This is because the dominant diagram with radiation from the muon vanishes when only left-handed photons are considered and because the chiral counting rules of HBChPT select only the pion poles in the leading order contribution from the other diagrams. Thus these observables include the various ingredients of the problem in a somewhat different way than does the unpolarized spectrum and so their measurement may help resolve the current disagreement between theory and experiment based just on the unpolarized spectrum.

The measurement of polarized photons in RMC on the proton is technically extremely challenging. The spectrum of left-handed photons is only one order of magnitude smaller than that of the unpolarized photons. However to measure the polarization of the photon one needs an additional scattering through an electromagnetic interaction or alternatively needs to measure the angular distributions of the electron-positron pair produced when the photon is stopped. Hence to obtain the same order of precision as that of an unpolarized RMC experiment, the polarization experiment must accumulate more events, say by as much as four orders of magnitude, than the unpolarized experiment. Such measurement is probably impossible with current muon beams and techniques, but may become feasible with the very intense muon beams which are now being discussed.



One should also note that there is an alternative quantity which could be measured, namely the angular asymmetry of the photon relative to the muon spin. By virtue of the general theorem of Ref. [26] this quantity has generally the same features and sensitivities as does  $\beta$ . It is much easier to measure, since one does not need to rescatter the photon, and in fact has been measured in nuclei [33]. However in the case of the proton, the muon loses almost all of its initial polarization as it is captured into atomic orbit. Hence the suppression factor, due now to the low residual polarization of the muon, may be just as large as for the polarized photon observables we have considered here.

On the other hand, in nuclei the capture rate for RMC increases proportional to  $Z^4$ , where  $Z$  is the number of protons in the nucleus. This makes measurements of the unpolarized rate in nuclei relatively easy [34,35]. So it may be feasible to measure the polarized photon observables in RMC on heavy nuclei. Indeed, the pion pole still gives the leading contribution and the general features remain the same, although there are the not insignificant complications in both calculations and interpretation introduced by the nuclear structure.

## VI. ACKNOWLEDGMENTS

We would like to thank M. Rho for his comments and helpful discussions. SA thanks T.-S. Park, F. Myhrer, and K. Kubodera for comments and discussions. DPM is very grateful to V. Vento for his warm hospitality during his stay at University of Valencia. This work is supported in part by Korea BK21 program, by KOSEF 1999-2-111-005-5 and KRF Grant No. 2000-015-DP0072, by NSF Grant No. PHY-9900756 and INT-9730847, and by the Natural Sciences and Engineering Research Council of Canada.

- 
- [1] G. Jonkmans *et al.*, Phys. Rev. Lett. **77** (1996) 4512; D. H. Wright *et al.*, Phys. Rev. **C 57** (1998) 373.
  - [2] V. Bernard, N. Kaiser and U.-G. Meißner, Phys. Rev. **D 50** (1994) 6899.
  - [3] H. W. Fearing, R. Lewis, N. Mobed and S. Scherer, Phys. Rev. **D 56** (1997) 1783.
  - [4] S. Ando and D.-P. Min, Phys. Lett. **B 417** (1998) 177.
  - [5] T. Meissner, F. Myhrer and K. Kubodera, Phys. Lett. **B 416** (1998) 36.
  - [6] G. I. Opat, Phys. Rev. **134** (1964) B428.
  - [7] H. W. Fearing, Phys. Rev. **C 21** (1980) 1951.
  - [8] M. Gmitro and A. A. Ovchinnikova, Nucl. Phys. **A 356** (1981) 323.
  - [9] D. S. Beder and H. W. Fearing, Phys. Rev. **D 35** (1987) 2130.
  - [10] D. S. Beder and H. W. Fearing, Phys. Rev. **D 39** (1989) 3493.
  - [11] H. W. Fearing, R. Lewis, N. Mobed, and S. Scherer, Nucl. Phys. **A 631** (1998) 735c.
  - [12] V. Bernard, H. W. Fearing, T. R. Hemmert, and U.-G. Meißner, Nucl. Phys. **A 635** (1998) 121; erratum **A 642** (1998) 563.
  - [13] J. Smejkal, T. Truhlík, and F. C. Khanna, Few Body Syst. **26** (1999) 175.
  - [14] V. Bernard, T. R. Hemmert, and U.-G. Meißner, Nucl. Phys. **A 686** (2001) 290.
  - [15] E. Truhlík and F. C. Khanna, nucl-th/0102006.
  - [16] I.-T. Cheon and M. K. Cheoun, nucl-th/9811009 v2.
  - [17] H. W. Fearing, nucl-th/9811027 v2.
  - [18] S. Ando, F. Myhrer, and K. Kubodera, Phys. Rev. **C 63** (2001) 015203.
  - [19] A. Halpern, Phys. Rev. **135** (1964) A34.
  - [20] D. D. Bakalov, M. P. Faifman, L. I. Ponomarev, and S. I. Vinitzky, Nucl. Phys. **A 384** (1982) 302.
  - [21] T. Gorringer, private communication.
  - [22] G. Bardin *et al.*, Nucl. Phys. **A 352** (1981) 365.
  - [23] G. Bardin *et al.*, Phys. Lett. **B 104** (1981) 320.
  - [24] D. V. Balin *et al.*, PSI proposal R-97-05.1 (Dec. 1996).
  - [25] R. Cutkosky, Phys. Rev. **107** (1957) 330; K. Huang, C. N. Yang, and T. D. Lee, Phys. Rev. **108** (1957) 1340; J. Bernstein, Phys. Rev. **115** (1959) 694; G. K. Manacher and L. Wolfenstein, Phys. Rev. **116** (1959) 782.
  - [26] H. W. Fearing, Phys. Rev. Lett. **35** (1975) 79.
  - [27] R. S. Sloboda and H. W. Fearing, Nucl. Phys. **A 340** (1980) 342.
  - [28] H. Georgi, Phys. Lett. **B 240** (1990) 447; E. Jenkins and A. Manohar, Phys. Lett. **B 255** (1991) 558.
  - [29] J. E. Donoghue, E. Golowich, and B. R. Holstein, *Dynamics of the standard model*, Cambridge Univ. Press (1992).
  - [30] G. Ecker, J. Gasser, A. Pich, and E. de Rafael, Nucl. Phys. **B 321** (1989) 311.
  - [31] H. W. Fearing, T. R. Hemmert, R. Lewis, and C. Unkmeir, Phys. Rev. **C 62** (2000) 054006.

- [32] G. Ecker and M. Mojžiš, Phys. Lett. **B 365** (1996) 312.
- [33] C. J. Virtue *et al.*, Nucl. Phys. **A517** (1990) 509, and references cited therein.
- [34] D. S. Armstrong *et al.*, Phys. Rev. **C 46** (1992) 1094.
- [35] P. C. Bergbusch *et al.*, Phys. Rev. **C 59** (1999) 2853.